

# Performance of Weighted Random Reference Patterns on Wireless Channel Model for Gesture Recognition

Yung-Fa Huang,<sup>1</sup> Hua-Jui Yang,<sup>2</sup> Yung-Hoh Sheu,<sup>3\*</sup> and Ching-Mu Chen<sup>4\*\*</sup>

<sup>1</sup>Department of Information and Communication Engineering, Chaoyang University of Technology, 168, Jifeng E. Rd., Wufeng District, Taichung 413310 Taiwan, R.O.C.

<sup>2</sup>Department of Information and Communication Engineering, Chaoyang University of Technology, 168, Jifeng E. Rd., Wufeng District, Taichung 413310 Taiwan, R.O.C.

<sup>3</sup>Department of Computer Science and Information Engineering, National Formosa University, Taiwan, No. 64, Wunhua Rd., Huwei Township, Yunlin County 632, Taiwan R.O.C.

<sup>4</sup>Department of Electrical Engineering, National Penghu University of Science and Technology, No. 300, Liuhe Rd., Magong City, Penghu County 880011, Taiwan R.O.C.

(Received December 12, 2023; accepted April 12, 2024)

**Keywords:** wireless sensor network, received signal strength, channel model, gesture recognition, weighted random reference pattern

In recent years, wireless sensor devices have become able to perform multiple functions such as detecting human sleep conditions, blood pressure, heartbeat, and running paths. We use the wireless channel model of a wearable Zigbee wireless sensing node to conduct research on human posture recognition. The received signal strength indicator (RSSI) obtained through the transmission and reception of wireless signals is used to obtain the model of the wireless channel. The wireless sensor nodes receive different RSSI patterns of human gesture based on which they recognize a gesture through their respective wireless channels by performing distance processing on the collected signal data. However, in this paper, we propose a weighted random reference pattern (WRRP) to achieve a higher recognition accuracy. Experimental results show that WRRP can achieve a recognition accuracy of 98%.

## 1. Introduction

The wireless sensor network (WSN) uses wireless sensor nodes to monitor the surrounding environment and collect information, such as the signal strengths of buildings, roads, and human bodies, which is transmitted back to WSN through wireless network technology.<sup>(1–6)</sup> The wireless sensors used in WSN include devices such as a wireless communication module, a control circuit, a CPU, and a power supply unit. Therefore, WSN can be used in, for example, military, medical, livelihood, industry, and transportation applications.<sup>(7)</sup>

With the advancement of technology, the application of WSN to human gesture sensing has become a hot topic.<sup>(6,8–11)</sup> Wireless sensor nodes have the advantages of small size, low cost, low power consumption, and easy network deployment. They can be used in the fields of livelihood, such as environmental and agricultural monitoring, home health care monitoring of the elderly,

---

\*Corresponding author: e-mail: [yhsheu@nfu.edu.tw](mailto:yhsheu@nfu.edu.tw)

\*\*Corresponding author: e-mail: [t20136@gms.npu.edu.tw](mailto:t20136@gms.npu.edu.tw)

<https://doi.org/10.18494/SAM4818>

industrial automation, and traffic control monitoring. Currently, Google Maps can be used for the outdoor application; however, WSN can also be used for indoor environments.

The human body area network can use the ZigBee transmission technology to monitor the dynamic-related information of human gestures, such as health-related information and other data.<sup>(12–14)</sup> The relevant information and data can be processed and analyzed to understand the physical condition of a human gesture, such as blood pressure or falls.<sup>(14,15)</sup> The body sensor network uses a small number of wireless sensor nodes and a small sensing area to provide data for specific medical care.<sup>(3–4,7)</sup> The body sensor network can be minimized, which will facilitate the transmission between nodes and reduce other network interferences.<sup>(14,16,17)</sup> In this study, we use wireless sensor nodes combined with detection devices for human body sensing and recognition. After collecting relevant data through wireless sensor nodes, recognition results are transmitted back to WSN through ZigBee.

A wireless body area network (WBAN) comprises many sensors connected to each other on a human body. To acquire data via WBAN, wireless sensor nodes are placed on a human body. Whenever the wearer moves, signals are sent to the heads of wireless sensor nodes and data are sent back to the base station to be used in decision-making. We carry out distance processing on the collected signal data to identify the human gesture. Moreover, the wireless sensor nodes generate different received signal strength indicator (RSSI) patterns for different human gestures, enabling a gesture to be identified on the basis of the wireless channel by performing distance processing on the collected signal data. In this paper, we propose a weighted random reference pattern (WRRP) to improve recognition. Experimental results show that WRRP can achieve a recognition accuracy of 98%.

## 2. Literature Review

Human body sensing and recognition can be analyzed and identified through image recognition and other technologies.<sup>(18,19)</sup> In wireless communication, the transmission environment cannot be ideal since there are many obstacles in the transmission environment. Signals in wireless communication are transmitted through a transmitter. Because of the presence of obstacles, the received signal might differ from the transmitted signal. For the receiving wireless sensor node, there may be a line-of-sight signal affected by reflection, as shown in Fig. 1. Such an affected signal will cause changes in the amplitude and phase of the transmitted signal. Signals arrive at the receiving wireless sensor nodes through different paths, whereby multiple signals with different delay times will have additive effects or destructive weakening effects on each other, thus causing the multipath fading phenomenon.<sup>(1–3)</sup> Some of the signals are sent directly to the destination, but other signals may reach the destination after being reflected by the obstacles. The result is that some signals are delayed and take a longer time to reach the destination.

Human body sensing and recognition are a biological behavior characteristic with a dynamic characteristic pattern that changes with time, so human body sensing and recognition are relatively unstable. Moreover, in image recognition, cameras are used to capture human body gestures and then the obtained data are calculated and processed. In addition, wireless sensors

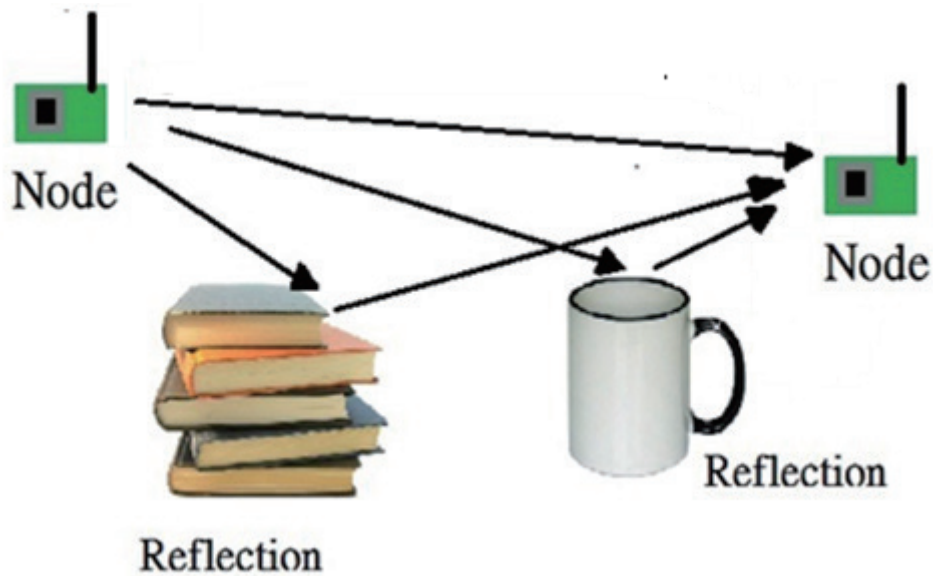


Fig. 1. (Color online) Multipath transmission environment.

are also used for human body sensing and recognition.<sup>(20,21)</sup> We use RSSI to establish a reference pattern for recognition. Most of the wireless sensors used are three-axis accelerometer sensors, which can use the three-axis changes in the sensed data to identify the difference in posture.<sup>(22–26)</sup>

Image recognition involves the use of a camera to capture the posture of the human body and the calculation and processing of the data to determine the posture. A camera with a single lens is used for 2D image recognition. There are also dual-lens cameras and infrared models used to measure the distance and depth of the human body for 3D image recognition. Moreover, there are also some image recognition methods that use wearable objects for gesture recognition.<sup>(21,27)</sup>

Furthermore, human bodies interact with each other on the basis of hand gestures that can be applied in many fields such as the study of body language. Therefore, how to recognize a human gesture is becoming increasingly important.<sup>(28–30)</sup> Wireless sensors are placed on different locations of a human body to understand what actions a person is performing in order to prevent risks. Furthermore, the symptoms or signals captured from a human body may be used to identify various events that might be occurring, such as an elderly man falling down. To prevent such events, wireless sensor nodes can be placed on a human body to capture data and send signals back to the base station. For example, emergency data provided by an elderly person in a wearable device can be used to prevent the risk before falls and to perform distance processing on the collected signal data to recognize human gestures. There are ways to recognize human activities, such as using sensors and image processing. There have been related studies on image processing.<sup>(31–34)</sup>

### 3. Weighted Random Reference Pattern Method

The main procedures and methods used are training, feature pattern extraction, reference pattern establishment, test of program, feature pattern extraction, pattern comparison, and majority decision to achieve a higher recognition rate. The wireless sensor nodes are used to measure signal data, and signals are extracted to select characteristic patterns. Then, the extracted signals are averaged to establish reference patterns for calculation. Because of the uncertainty of dynamic signals, time, climate, the location of items, and multipath fading will affect experimental data. For a more accurate analysis of the experimental results, the reference pattern signal is divided into  $n$  pairs, and we use  $n, n-2, n-4, n-6 \dots$  pairs for comparison. The characteristic patterns are extracted from the signals and converted into test pattern signals. Assuming that there are 10 pairs of signals, a few pairs will be selected for pattern comparison.

Assuming that  $n$  pairs of reference pattern signals are extracted, other  $n$  pairs of signal data different from the previous pairs are extracted as the 1st group of test patterns for comparison. Then, the 3rd group of  $n$  pairs of signal data different from the 2nd group are extracted and used as the 2nd group of test patterns, the 4th group of  $n$  pairs of signal data different from the 3rd group are extracted and used as the 3rd group of test patterns, and so on. There will be  $n+1$  sets of test patterns from  $n$  pairs for later analysis and comparison, and the other  $n-2, n-4, n-6$ , and 1 pairs will also make up  $n+1$  sets of patterns.

Typically, nine pairs of reference pattern signals are compared for 100 data judgments. Seven pairs of reference pattern signals are compared for 300 data judgments. Five pairs of reference pattern signals are compared for 500 data judgments. Three pairs of reference pattern signals are compared for 700 data judgments. One pair of reference pattern signals is compared for 900 data judgments. After the majority vote, the system carries out the final processing of recognition results, that is, nine pairs, seven pairs, five pairs, three pairs, and one pair of reference patterns are identified for recognition results. Figure 2 shows the recognition flowchart where the difference in signal distribution is used to investigate reference patterns for body movement recognition.

When  $p$  pairs of signals take  $x$  actions in several pairs, each action will have  $n$  sampling data, and the average of each pair, used as the reference value for analysis, is expressed as

$$X_{p,l} = \{X_{p,l}[1]X_{p,l}[2] \dots X_{p,l}[n] \dots X_{p,l}[N]\}, \quad (1)$$

where  $X_{p,l}$  is the RSSI test pattern obtained for the  $p$  pair for  $l$  number of times.

The patterns are divided into two types: test pattern  $X_p$  and reference pattern  $Y_p$ . The reference pattern is expressed as

$$Y_p = \frac{1}{L} \sum_{l=1}^L X_{p,l}, \quad (2)$$

where  $Y_p$  is obtained by taking  $X_{p,l}$  as the  $p$  pair of RSSI test patterns acquired at the  $l$  time.

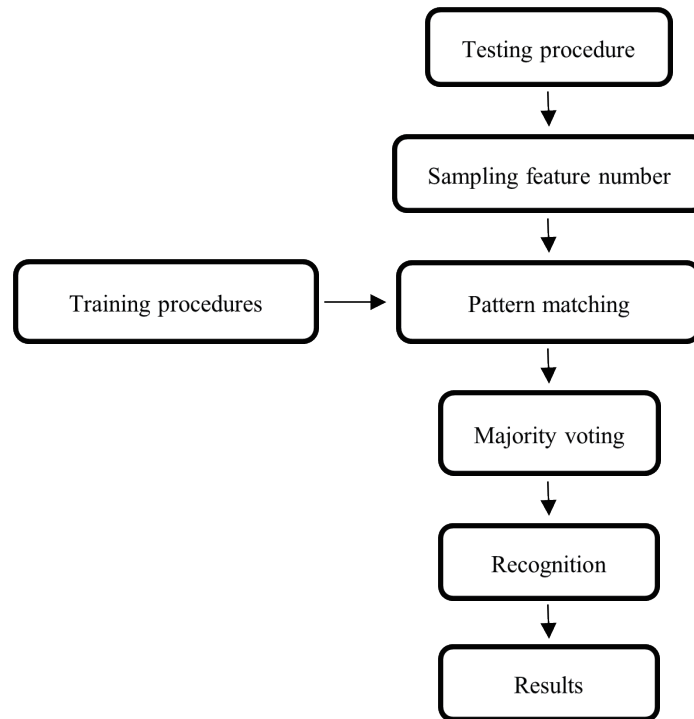


Fig. 2. Recognition flowchart.

The distance  $d$  is obtained by subtracting  $Y_p$  and  $X_p$ , taking the square and the root sign as

$$d = (Y_p - X_p) = \sqrt{(y_p - x_p)(y_p - x_p)^T}, \quad (3)$$

where  $d$  is the distance between  $Y_p$  and  $X_p$ . However, the results of analyzing and calculating the test and reference patterns using Eq. (3) show that the smaller the distance  $d$ , the higher the probability of human body movement recognition.

Therefore, the weights assigned to the  $n$  pattern values in 4 s are expressed as

$$w_m = \text{Diag}\{w_m[1] w_m[2] \dots w_m[i] \dots w_m[n]\}, \quad (4)$$

where  $w_m$  is the  $m$ th weight and  $\text{Diag}\{\}$  is an array.

The distance with weights can be expressed by

$$d_{pw} = (Y_p - X_p) = \sqrt{(y_p - x_p)w_m(y_p - x_p)^T}, \quad (5)$$

where  $d_{pw}$  is a distance combined with  $w_m$ .

After the step of extracting feature patterns, the next step is pattern matching. The reference pattern signal is used for distance calculation using Eq. (3), and the calculated distances are then

compared. Each pair of reference patterns is divided into horizontal and vertical reference patterns. Therefore,  $d$  will have two values after each test pattern comparison. More precisely, since the human body sensing measured using  $2d$  is better, a good value of  $d$  will be relatively small. If there are seven pairs of reference pattern signals, the three remaining pairs are the test signals for distance calculation. If there are five pairs of reference pattern signals, the five remaining pairs are the test signals for distance calculation.

The majority voting process is performed on the values of each group. The majority decision is adopted to improve the accuracy of recognition. Assuming that there are seven pairs of reference patterns in each set of values, the pattern comparison will compare seven values to see if there are better actions. If five of the seven values are judged as correct, the group is judged to be correct, which can also be correct once. On the contrary, if fewer than four of the seven values are correct, this group is judged to be an error.

#### 4. Simulation Results

We use the ZigbeX system as a simulator for calculating both vertical and horizontal body movements. The ZigbeX system is composed of software, a microcontroller (ATmega128L), a wireless communication chip (CC2420), a sensor, and an antenna.<sup>(22,31)</sup> There are two types of movement recognition action in this experiment as shown in Fig. 3. The first type is raising the arm vertically until the arm is parallel to the body. The second type of movement action is moving the arm horizontally. The data measured are divided into ten pairs of signal patterns. Each pair (day) consists of five vertical movements and five horizontal movements, a total of ten times per day for a total of 100 times in ten days. Each action has a movement time of 4 s and is

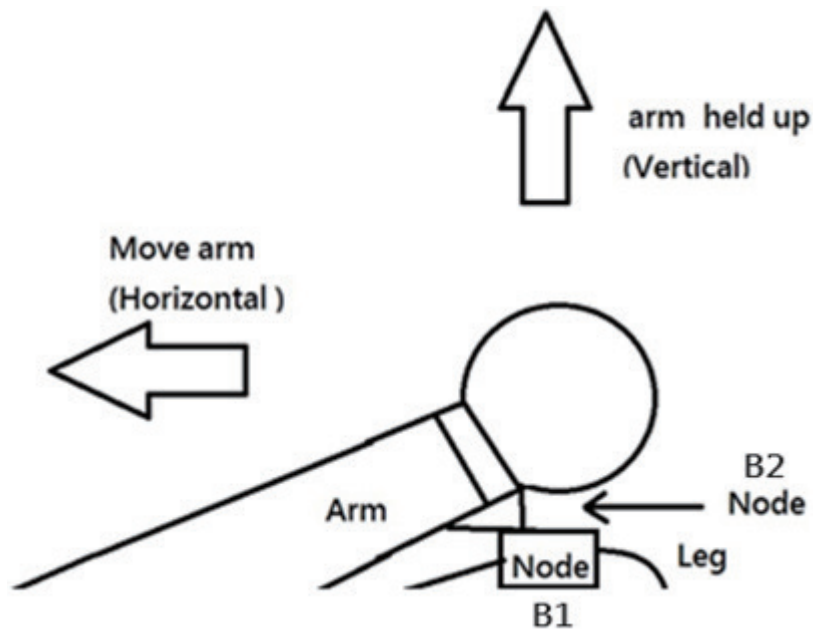


Fig. 3. Schematic diagram of the operation process.

sampled every 0.5 s. The speed of arm movement is about  $20 \text{ cm}\cdot\text{s}^{-1}$ . The reference database for this experiment consists of 10 data values from the P1R1 database, where P stands for people and R stands for rounds. These 10 data values are the average dBm values of each day for 10 pairs. The test patterns are the measurement data of P1R2, P2, and P3. The reference for reference comparison analysis in this experiment is the logarithm of RP. Among the 10 pairs of patterns, the horizontal and vertical distances are each set to 1, 2, 3, 4, 5, 6, 7, 8, 9, and 10. If the reference pattern is one pair, take the 9 pairs of test patterns. If the reference pattern is five pairs, take the 5 pairs of test patterns. When there is one pair of reference patterns, there will be 90 majority comparisons. When there are three pairs of reference patterns, there will be 70 majority comparisons. When there are five pairs of reference patterns, there will be 50 majority comparisons. When there are seven pairs of reference patterns, there will be 30 majority rule comparisons, and when there are nine pairs of reference patterns, there will be 10 majority rule comparisons.

In this study, we use two wireless sensor nodes, where the receiving node B1 is placed on the left leg of the subject. The other node B2 is worn under the left wrist of the subject. At the start, the distance between these two wireless sensor nodes is about 1 cm. These two wireless sensor nodes move at a speed of about  $20 \text{ cm}\cdot\text{s}^{-1}$  to collect the signals used for recognition, as shown in Fig. 3.

Figure 4 shows the dynamic signal distribution of B2 horizontal movement. The distributions of the 10 pairs of signal values are similar. Among them, the dotted line of the 8th pair reaches  $-45 \text{ dBm}$  in the next 2.5 to 4 s, and all values decrease from  $-25$  to  $58 \text{ dBm}$ .

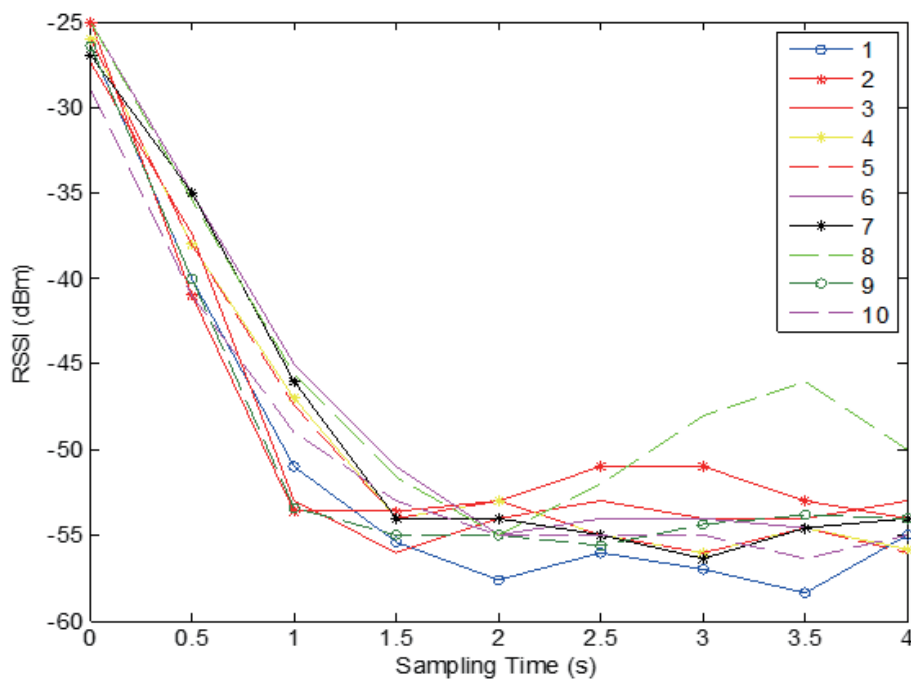


Fig. 4. (Color online) Horizontal distribution diagram.



Figure 5 shows the dynamic signal distribution of B2 vertical movement. The RSSI value of the horizontal part drops from  $-46$  to  $53$  dBm in the first second. The RSSI value of the vertical part is from  $-43$  to  $54$  dBm. From 2 to 4 s, the RSSI values of the horizontal and vertical parts decrease to  $-55$  dBm.

In Figs. 4 and 5, the main difference between the horizontal and vertical signal distributions is seen between 2 and 4 s. Therefore, if only the signal from 2 to 4 s is extracted as a pattern, the signal recognition rate can be used. However, the weights determined using Eq. (4) will be assigned to the  $n$  sampled values in 4 s. The horizontal and vertical distributions of one of the 10 pairs are selected for discussion, as shown in Fig. 6. The solid line H2 is the horizontal distribution and the dotted line V1 is the vertical distribution. There is little difference between the dynamic signals of the horizontal and vertical movements.

The data of PIR1 itself is used as the reference pattern. Three weights ( $w_m$ ) are used, 00001111, 000111000, and 11110000, as shown in Table 1. The weight sum is used for WRRP identification and analysis. The analysis results of PIR1 using itself as a reference pattern for weight summation are shown in Fig. 7. The analysis results show that the accuracy of Type N weights is higher than those of Types E and I weights. Figure 8 shows the accuracy rate for the recognition results. The horizontal axis is the reference pattern signal and the vertical axis is the accuracy rate of recognition. The results show that the reference pattern proposed in this paper has a recognition accuracy of 98%.

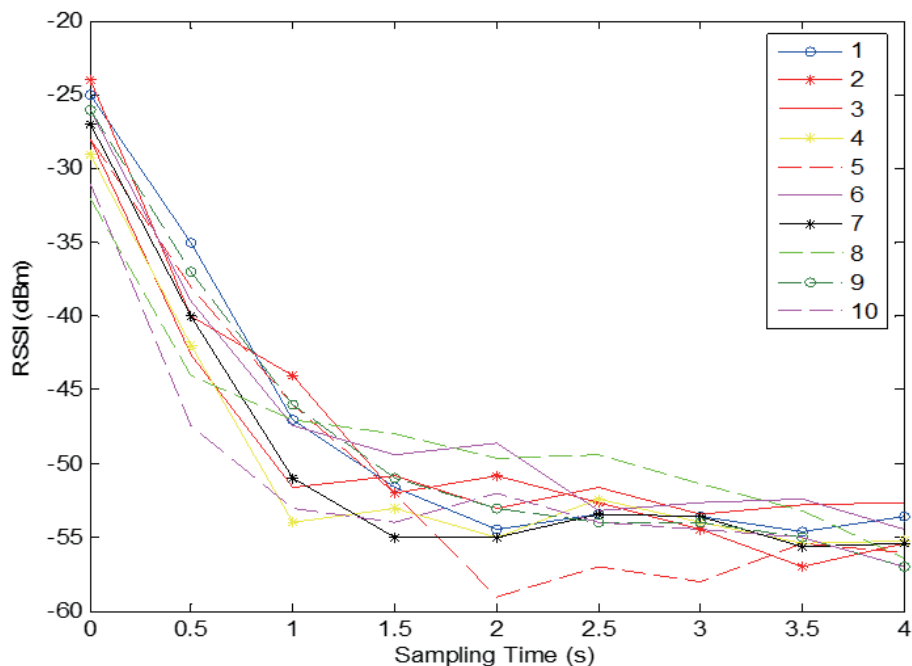


Fig. 5. (Color online) Vertical distribution diagram



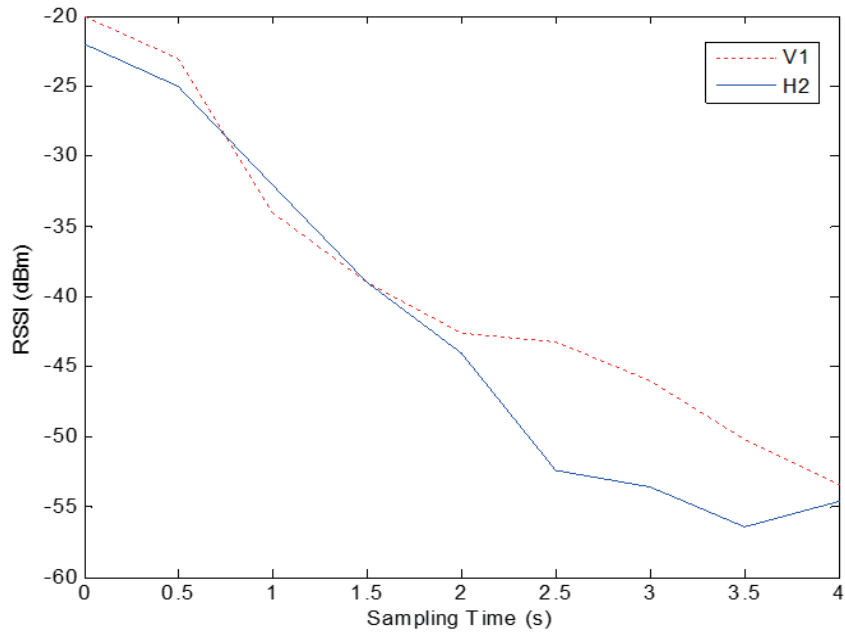


Fig. 6. (Color online) Horizontal and vertical signal patterns of one pair out of the 10 pairs of P1R1.

Table 1  
Types of weight ( $w_m$ ).

Type N	Type E	Type I
0,0,0,0,1,1,1,1,1	0,0,0,1,1,1,0,0,0	1,1,1,1,1,0,0,0,0

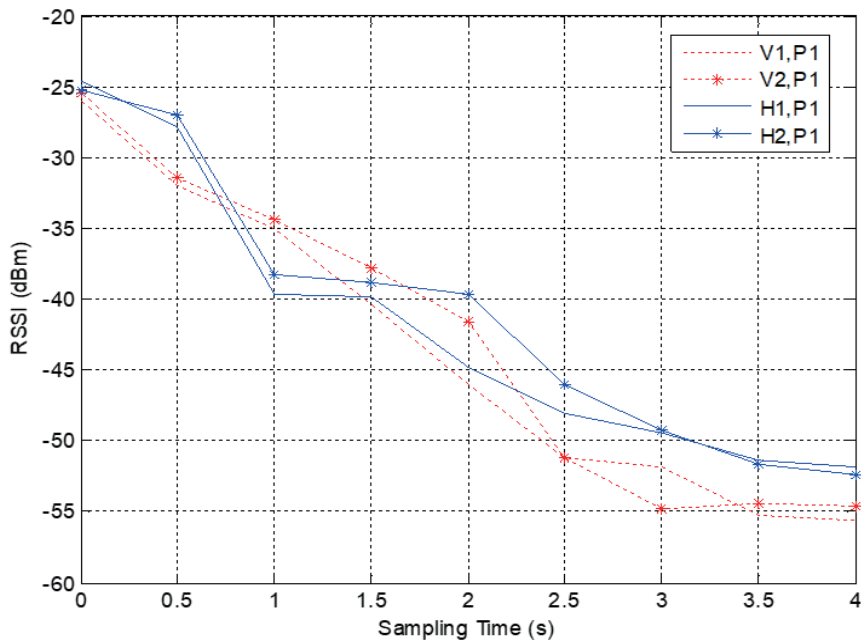


Fig. 7. (Color online) One pair of horizontal and vertical signal patterns out of the 10 pairs of P1R2.

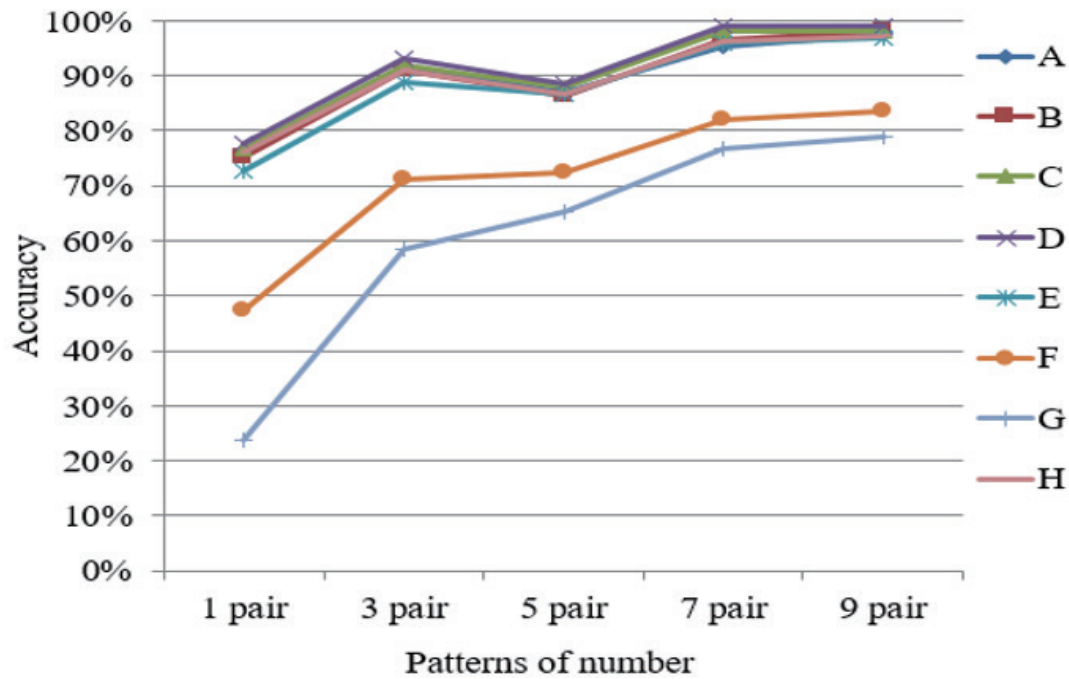


Fig. 8. (Color online) Accuracies obtained using various weighting patterns.

In Figs. 6 and 7, V1 is for horizontal motion and H2 is for vertical motion. The main difference between the horizontal and vertical signal distributions is seen in the distribution from 2 to 4 s. Therefore, if only the signal from 2 to 4 s is extracted as a pattern, the signal recognition rate can be discussed for signals of recognition rate. The effects of different weight distribution characteristics on the recognition rate will be designed. The weights determined using Eq. (4) are assigned to the nine pattern values in 4 s, and  $n$  is set as 9. There will be different weight sets, A, B, C, D, E, F, G, and H, as shown in Table 2, calculated using Eq. (4). According to Table 3, the test pattern for identification analysis is PIR1. However, the result of the reference pattern shows that PIR1 is better than PIR2 as shown in Table 3. The results obtained with the weight categories A, B, C, D, E, F, G, and H are shown in Table 4. If the weight of the later pattern values is increased, the accuracy rate will be higher, as we expected, than the other weights.

The results of weight categories are shown in Fig. 8. In Table 2, the weight categories gradually decrease or increase on the right side of B and C, revealing the effect of the weight distribution on the identification. In Table 4, the recognition accuracy of the weight category D is the highest. This is because the weight of category D placed on the last four samples has a large difference between the horizontal and vertical signals in the last part of movements. A change in weight distribution will affect the identification results. The experimental recognition results show that using WRRP as a reference pattern improves the recognition accuracy. Experimental results show that the WRRP proposed in this paper led to a recognition accuracy of 98%.

Table 2  
Weights for different categories ( $w_m$ ).

Category	$w_m$
A	1,1,1,1,1,1,1,1
B	0.9,0.8,0.7,0.6,0.5,0.4,0.3,0.2,0.1
C	0.1,0.2,0.3,0.4,0.5,0.6,0.7,0.8,0.9
D	0,0,0,0,1,1,1,1
E	0,0,0,1,1,0,0,0
F	1,1,1,1,0,0,0,0
G	1,1,1,0,0,0,0,0
H	0,0,0,1,1,1,0,0

Table 3  
Recognition results for reference pattern and a number of reference patterns.

Reference pattern	Number of reference patterns (pairs)				
	9	7	5	3	1
PIR1	98.0%	95.3%	87.0%	91.5%	76.2%
PIR2	95.0%	67.0%	60.0%	51.6%	37.4%

Table 4  
Weight analysis results with reference pattern.

Category	Number of reference patterns (pairs)				
	9	7	5	3	1
A	97.5%	95.3%	87.0%	91.5%	76.2%
B	98.0%	96.7%	86.2%	91.0%	75.2%
C	98.0%	98.0%	87.8%	92.0%	76.8%
D	99.0%	99.0%	88.6%	93.3%	77.6%
E	97.0%	96.0%	86.8%	88.7%	72.7%
F	98.5%	96.7%	86.4%	88.7%	74.3%
G	93.0%	92.0%	83.0%	84.9%	71.8%
H	97.3%	96.3%	86.6%	91.0%	76.1%

## 5. Conclusions

In this paper, we proposed WRRP by using Zigbee wireless sensor nodes for human body gesture recognition. Owing to the fact that sample signals of a gesture differ for the beginning and ending movements, we set different weights from 0 to 1 for weighting different samples. Experimental recognition results show that the proposed WRRP improved the recognition accuracy of 98%. Moreover, the weight of category D placed on the last four samples even showed a large difference between the horizontal and vertical signals in the last part of movements with a recognition accuracy of 99%.

## Acknowledgments

This research was supported by the National Science and Technology Council (NSTC), Taiwan, with grant number NSTC 113-2425-H-028-003. The project is part of Integration of Information Technology and Sports Medicine in Intelligent Table Tennis: From Taiwan to International Perspectives.

## References

- 1 S. L. Cotton and W. G. Scanlon: IEEE Trans. Commun. Mag. **47** (2009) 78. <https://doi.org/10.1109/MCOM.2009.5273811>
- 2 S. L. Cotton and W. G. Scanlon: IEEE Int. Symp. Personal, Indoor and Mobile Radio Communications (2006) 1. <https://doi.org/10.1109/PIMRC.2006.254266>
- 3 R. D. Errico and L. Ouvry: IEEE Int. Symp. Personal, Indoor and Mobile Radio Communications (2009) 3000. <https://doi.org/10.1109/PIMRC.2009.5449948>
- 4 S. S. Rautaray and A. Agrawal: Artif. Intell. Rev. **43** (2015) 1. <https://doi.org/10.1007/s10462-012-9356-9>
- 5 M. Kim and J. Takada: IEEE Int. Symp. Antennas and Propag. Soc. (2009) 1. <https://doi.org/10.1109/APS.2009.5172162>
- 6 N. M. Mohamed, B. Mustafa, and N. Jomhari: IEEE Access **9** (2021) 157422; <https://doi.org/10.1109/ACCESS.2021.3129650>
- 7 Q. H. Abbasi, A. Sani, A. Alomainy, and H. Yang: IEEE Trans. Inf. Technol. Biomed. **16** (2012) 221. <https://doi.org/10.1109/TITB.2011.2177526>
- 8 C. Bachmann, M. Ashouei, V. Pop, M. Vidojkovic, H. D. Groot, and B. Gyselinckx: IEEE Commun. Mag. **50** (2012) 20. <https://doi.org/10.1109/MCOM.2012.6122528>
- 9 S. Mitra and T. Acharya: IEEE Trans. Systems, Man, and Cybern. Part C Appl. Rev. **37** (2007) 311. <https://doi.org/10.1109/TSMCC.2007.893280>
- 10 F. Palumbo, C. Gallicchio, R. Pucci, and A. Micheli: J. Ambient Intell. Smart Environ. **8** (2016) 87. <https://doi.org/10.3233/AIS-160372>
- 11 J. A. Rocha, G. Piñeres-Espitia, S. A. Butt, E. De-la-Hoz-Franco, M. I. Tariq, D. C. Sinito, and Z. Comas-González: Int. Conf. Adv. Intell. Data Anal. Appl. Smart Innovation, Syst. Technol. **253** (2021) 327. [https://doi.org/10.1007/978-981-16-5036-9\\_31](https://doi.org/10.1007/978-981-16-5036-9_31)
- 12 M. A. Hanson, H. C. Powell, A. T. Barth, K. Ringgenberg, B. H. Calhoun, J. H. Aylor, and J. Lach: Computer **42** (2009) 58. <https://doi.org/10.1109/MC.2009.5>
- 13 T. Zasowski, F. Althaus, M. Stager, A. Wittneben, and G. Troster: IEEE Conf. Ultra Wideband Syst. Technol. (2003) 285. <https://doi.org/10.1109/UWBST.2003.1267849>
- 14 R. D'Errico, R. Rosini, and M. Maman: IEEE Int. Conf. Commun. (2011) 1. <https://doi.org/10.1109/icc.2011.5962980>
- 15 M. Momoda and S. Hara: J Wireless Commun. Network **2015** (2015) 238. <https://doi.org/10.1186/s13638-015-0459-2>
- 16 D. B. Smith and D. Miniutti: IEEE Wireless Communications and Networking Conf. (2012) 689. <https://doi.org/10.1109/WCNC.2012.6214457>
- 17 M. Kim, K. Wangchuk, and J. I. Takada: 6th European Conf. Antennas and Propagation (2012) 548. <https://doi.org/10.1109/EuCAP.2012.6206638>
- 18 Z. Ren, J. Yuan, J. Meng, and Z. Zhang: IEEE Trans. Multimedia **15** (2013) 1110. <https://doi.org/10.1109/TMM.2013.2246148>
- 19 L. K. Phadtare, R. S. Kushalnagar, and N. D. Cahill: Western New York Image Processing Workshop (2012) 29. <https://doi.org/10.1109/WNYIPW.2012.6466652>
- 20 R. Xu, S. Zhou, and W. J. Li: IEEE Sens. **12** (2012) 1166. <https://doi.org/10.1109/JSEN.2011.2166953>
- 21 R. L. Ashok and D. P. Agrawal: Computer **36** (2003) 31. <https://doi.org/10.1109/MC.2003.1244532>
- 22 O. Köpüklü, A. Gunduz, N. Kose, and G. Rigoll: IEEE Trans. Biom. Behav. Identity Sci. **2** (2020) 85. <https://doi.org/10.1109/TBIOM.2020.2968216>
- 23 A. K. Rajagopal, R. Subramanian, E. Ricci, R. L. Vieriu, O. Lanz, R. Kalpathi, and N. Sebe: Int. J. Comput. Vis. **9** (2014) 146. <https://doi.org/10.1007/s11263-013-0692-2>
- 24 G. Benitez Garcia, L. Prudente Tixteco, L. C. Castro Madrid, R. Toscano Medina, J. Olivares Mercado, G. Sanchez Perez, and L. J. G. Villalba: Sensors **21** (2021) 356. <https://doi.org/10.3390/s21020356>
- 25 N. Zengeler, T. Kopinski, and U. Handmann: Sensors **19** (2019) 59. <https://doi.org/10.3390/s19010059>
- 26 M. Asadi-Aghbolaghi, A. Clapés, M. Bellantonio, H. J. Escalante, V. Ponce-López, X. Baró, I. Guyon, S. Kasaei, and S. Escalera: The Springer Series on Challenges in Machine Learning (Springer, Cham., 2017) pp. 539–578. [https://doi.org/10.1007/978-3-319-57021-1\\_19](https://doi.org/10.1007/978-3-319-57021-1_19)
- 27 Z. Hu, Y. Hu, J. Liu, B. Wu, D. Han, and T. Kurfess: Neurocomputing **318** (2018) 151. <https://doi.org/10.1016/j.neucom.2018.08.042>
- 28 A. S. Phyo, H. Fukuda, A. Lam, Y. Kobayashi, and Y. Kuno: ICIC Lecture Notes in Computer Science (Springer, Cham., 2019) p. 43. [https://doi.org/10.1007/978-3-030-26766-7\\_5](https://doi.org/10.1007/978-3-030-26766-7_5)

- 29 E. Ohn-Bar and M. M.Trivedi: IEEE Trans. Intell. Transport. Syst. **15** (2014) 2368. <https://doi.org/10.1109/TITS.2014.2337331>
- 30 A. Joshi, C. Monnier, M. Betke, and S. Sclaroff: Image Vis. Comput. **58** (2017) 86. <https://doi.org/10.1016/j.imavis.2016.06.001>
- 31 N. K. N. Aznan and Y. M. Yang: Recent Development in Wireless Sens. and Ad-hoc Networks. Signals and Communication Technology (Springer). [https://doi.org/10.1007/978-81-322-2129-6\\_3](https://doi.org/10.1007/978-81-322-2129-6_3)
- 32 A. Poullose, J. H. Kim, and D. S. Han: Comput. Intell. Neurosci. **2022** (2022) 1. <https://doi.org/10.1155/2022/1808990>
- 33 U. Anitha, R. Narmadha, D. Sumanth Raja, and D. Naveen Kumar: Procedia Comput. Sci. **167** (2020) 870. <https://doi.org/10.1016/j.procs.2020.03.426>
- 34 T. Dobhal, V. Shitole, G. Thomas, and G. Navada: Procedia Comput. Sci. **58** (2015) 178. <https://doi.org/10.1016/j.procs.2015.08.050>

## About the Authors



**Yung-Fa Huang** received his B.S. degree in electrical engineering from National Taipei University of Technology in 1982, his M.S. degree in electrical engineering from National Tsing Hua University, Taiwan, in 1987, and his Ph.D. degree in electrical engineering from National Chung Cheng University, Taiwan, in 2002. From 2004 to 2007, he was an associate professor at the Graduate Institute of Networking and Communication Engineering, Chaoyang University of Technology, Taiwan. From 2007 to 2008, he was the department head of Computer and Communication Engineering and the institute chair of the Graduate Institute of Networking and Communication Engineering, Chaoyang University of Technology. From 2008 to 2010, he was the department head of Information and Communication Engineering, Chaoyang University of Technology. Since 2011, he has been a professor at the Department of Information and Communication Engineering, Chaoyang University of Technology. His current research interests include multiuser detection in OFDM-CDMA cellular mobile communication systems, communication signal processing, fuzzy systems, and wireless sensor networks. Dr. Huang is a member of IEEE and serves as a co-chair of the IEEE SMC Society Technical Committee on Intelligent Internet Systems. ([yfahuang@cyut.edu.tw](mailto:yfahuang@cyut.edu.tw))



**Yung-Hoh Sheu** received his Ph.D. degree in electrical engineering at the National Cheng Kung University, Taiwan. He is currently a professor at National Formosa University of Science and Technology, Taiwan. His research interests are in embedded systems, communication, and networks. Besides working as a professor, he is a college dean of Electrical and Computer Engineering. ([yhsheu@nfu.edu.tw](mailto:yhsheu@nfu.edu.tw))



**Ching-Mu Chen** received his Ph.D. degree from the National Changhua University of Education, Taiwan, in 2012. From Aug. 2023 to the present, he has been an assistant professor at National Penghu University of Science and Technology, Taiwan. Since 2012, he has specialized in the field of electrical engineering. His research interests are in WSNs and sensors.

[t20136@gms.npu.edu.tw](mailto:t20136@gms.npu.edu.tw)